

## Broadband Laser Emission from Color Centers Inside MgO Microcrystals

T. Uchino

*Department of Chemistry, Graduate School of Science, Kobe University, Kobe 657-8501, Japan*

D. Okutsu

*Department of Chemistry, Faculty of Science, Kobe University, Kobe 657-8501, Japan*

(Received 9 April 2008; published 11 September 2008)

We report room-temperature broadband laser emission in the near-ultraviolet to the blue-green spectral range using color centers in MgO microcrystals. The lasing MgO microcrystals are obtained through a solid phase reaction between SiO and Mg at 450 °C in an argon atmosphere and are mostly composed of an accumulation of microcubes enclosed by {100} facets. The laser action was observed in the wavelength region from 350 to 600 nm without using cavity mirrors. In the present MgO microcrystals, some of the color centers will be stabilized at the interfaces and/or boundaries of the microcrystalline domains, probably explaining the stable laser action even at room temperature.

DOI: [10.1103/PhysRevLett.101.117401](https://doi.org/10.1103/PhysRevLett.101.117401)

PACS numbers: 78.45.+h, 42.55.-f, 71.55.-i, 73.20.Hb

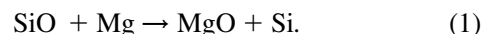
Since the electronic states of the color centers, which are electron (or hole) trapping defects in insulating crystals, are tightly coupled to the crystal phonons, the related optical transitions generally occur as wide and vibrationally broadened bands with a large ( $f > 0.1$ ) oscillator strength [1–4]. Thus, color centers are nearly ideal for the creation of efficient, optically pumped, broadly tunable lasers, as indeed realized in some alkali halide single crystals, for example, LiF, NaCl, and KF [5]. One disadvantage of this type of laser is that it generally requires cryogenic cooling to prevent destruction of the centers during laser action [2]. Furthermore, the tuning ranges of the alkali-halide-based color-center lasers are limited in the near-infrared region [2,5].

It was previously suggested that the  $F^+$  centers (oxygen vacancies each occupied by one electron) in alkaline-earth oxides are a great potential candidate for tunable solid-state lasers operating over a considerable part of the visible spectrum since the potential well of the color centers in alkaline-earth oxides are much deeper than those in alkali halides [2]. However, laser action using color centers in alkaline-earth oxides has been reported only for the  $F^+$  centers in CaO [6]. One principal barrier to explore laser action of the color centers in alkaline-earth oxides is the considerable difficulty in obtaining crystals of the highly refractory hosts [2]. The problem is so severe that no others have so far been able to reproduce the laser action reported in Ref. [6].

Another possible candidate for alkaline-earth-oxide-based tunable-laser materials is MgO [7]. However, introducing color centers in MgO is also difficult as in the case of CaO. Thermochemical reduction has often been used to produce a substantial amount of color centers ( $\sim 10^{17}/\text{cm}^3$ ) in MgO [8,9]; however, no laser action was reported even from the heavily reduced MgO single crystals.

In this Letter, we propose a rather simple method to prepare wideband tunable laser sources consisting of MgO

microcrystals. The proposed method utilizes the following reaction between Mg and silicon monoxide (SiO):



We found that the colored MgO microcrystals were obtained by heating the SiO/Mg mixture at 450 °C in argon atmosphere. We also found, for the first time, that the thus prepared MgO microcrystals exhibit room-temperature stimulated emission in the absence of cavity mirrors in short wavelength ranges of blue/green and near ultraviolet (UV).

To prepare the lasing MgO microcrystals pure Mg (99.9%,  $\sim 180 \mu\text{m}$ ) and SiO (99.99%,  $\sim 75 \mu\text{m}$ ) powders were used as starting materials. The SiO/Mg mixture of molar ratio 1:2 was thoroughly mixed and put in the alumina crucible. The crucible is closed with a 4-mm-thick alumina lid and placed in an electric furnace. The furnace was then evacuated to a pressure down to  $\sim 30$  Pa and purged with argon. The temperature of the furnace was raised to 450 °C at a rate of 7 °C/min and kept constant at 450 °C for 5 h under flowing argon environment. After the heating process, light gray powders were deposited onto the lid, and the blue-black substances were found in the bottom of the crucible. Powder x-ray diffraction (XRD) patterns of the resulting products were obtained with a diffractometer (Rigaku, RINT Ultima) using Cu  $K_\alpha$  radiation at ambient temperature. Scanning electron microscopy (SEM) and energy dispersive x-ray analysis (EDX) were conducted with a scanning electron microscope (JEOL, JSM-5610LVS) with energy dispersive spectrometer. Steady state photoluminescence (PL) spectra and the time-resolved PL signals in the millisecond to second time region were recorded on a spectrofluorometer (JASCO, FP 6600) using a xenon lamp for excitation. The internal quantum yield was estimated as the ratio of the emitted photons to the difference in the number of diffuse reflected photons from the sample and the non-

absorbing standard, according to the method described by Wrighton and co-workers [10]. We also estimated the external quantum yield, which is defined as the ratio of the emitted photons from the sample to the reflected photons from the nonabsorbing standard. As nonabsorbing standard, we used commercial micrometer-sized MgO powders [10], which do not normally have any absorption bands in the near-UV or visible region. We confirmed that the reflectivity of the standard is very similar to that of the sample at wavelengths where the sample does not show absorption ( $\lambda \sim 400$  nm). Time-resolved PL signals in the nanosecond region and the power-dependent PL emission were recorded at room temperature using the fourth harmonic (266 nm) of a pulsed Nd:YAG laser (pulse width 8 ns; a repetition rate 10 Hz) with a 150 lines/mm grating and a gated image intensifier CCD camera.

The XRD pattern of the light gray powders deposited onto the lid is shown in Fig. 1(a). We see from Fig. 1(a) that

the deposited powders consist mostly of MgO. A SEM image of the powders [see the inset of Fig. 1(b)] shows that there are well-defined {100} facets derived from the accumulated crystalline cubes on the order of a few micrometers. From the EDX analysis [see Fig. 1(b)], these cubes are identified as MgO. The existence of facets can be considered as evidence of relatively good crystallinity of the powder particles.

It should be worth mentioning that the deposition or sublimation of MgO occurs at a temperature well below the melting point of Mg ( $T_m = 650^\circ\text{C}$ ) or MgO ( $T_m = 2827^\circ\text{C} \pm 30^\circ\text{C}$ ). Although the liquidus compositions along the branch from the melting point of pure Mg to  $\text{MgO}_x$  ( $x < 1$ ) have not been well determined, the estimated melting point of  $\text{MgO}_x$  ( $x < 1$ ) is  $\sim 650^\circ\text{C}$  irrespective of the value of  $x$  [11]. Thus, it is quite likely that the oxides sublimate in the form of Mg and/or its suboxides.

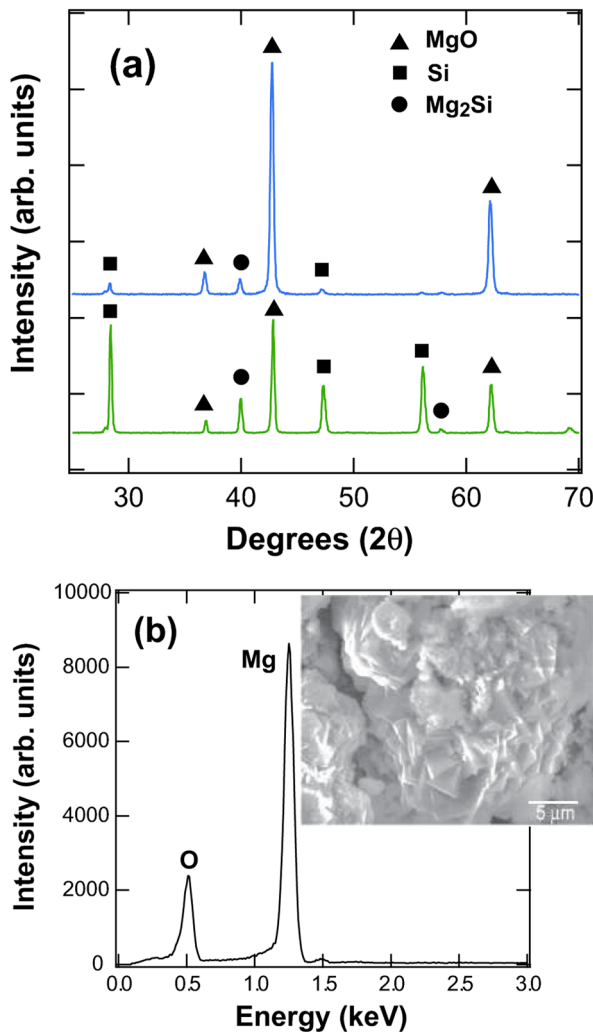


FIG. 1 (color online). (a) XRD patterns of the powders deposited onto the top lid (upper) and the materials found in the bottom of the crucible (lower). (b) An EDX spectrum of the microcube regions of the deposited powders. The inset shows a SEM image of the deposited powders.

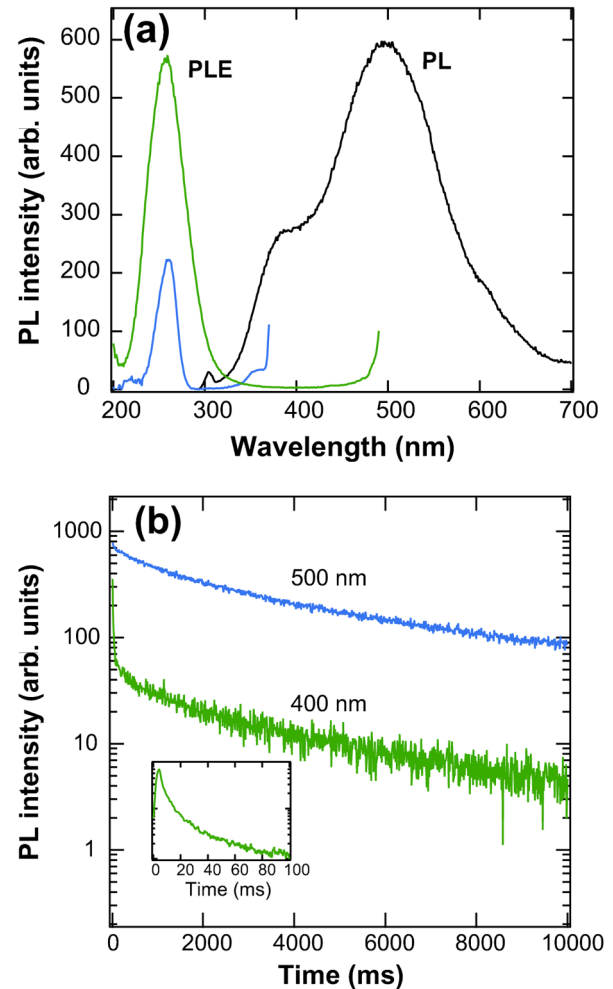


FIG. 2 (color online). PL characteristics of the MgO powders deposited onto the top lid. (a) Typical PL and PLE spectra. The excitation wavelength for the PL spectrum is 256 nm, while the monitor wavelengths of the PLE spectra are 500 nm (upper line) and 400 nm (lower line). (b) The PL decay curves monitored at 400 and 500 nm. The inset shows the expanded plot of the PL decay curve at 400 nm in the time region from 0 to 100 ms.

When the mixture of  $\text{SiO}_2$  and Mg (or only pure Mg) was similarly heated in an argon atmosphere at  $450^\circ\text{C}$ , none was deposited onto the top lid. This implies that the vaporization and the subsequent oxidation of Mg are not responsible for the deposition of MgO powders [12]. We suggest that the thermally induced disproportionation reaction of SiO [13,14], i.e.,  $2\text{SiO} \rightarrow \text{SiO}_2 + \text{Si}$ , plays a role in exhibiting such a low-temperature magnesiothermic reduction and the sublimation phenomenon.

The XRD pattern of the blue-black substances that remained in the bottom of the crucible is also shown in Fig. 1(a), demonstrating that they comprise MgO, Si, and  $\text{Mg}_2\text{Si}$ . This indicates that in addition to Eq. (1), the formation of magnesium silicide by, for example,  $\text{Si} + 2\text{Mg} \rightarrow \text{Mg}_2\text{Si}$ , also occurs in the present reaction processes.

Typical PL and PL excitation (PLE) spectra of the deposited MgO powders are shown in Fig. 2(a). We see that the sample is effectively excited by  $\sim 5\text{ eV}$  ( $\sim 250\text{ nm}$ ) photon, yielding two broad PL bands at  $\sim 400$  and  $\sim 500\text{ nm}$ . The internal and external quantum yields of this powdered sample measured with 256-nm excitation were  $11.2\% \pm 0.5\%$  and  $5.1\% \pm 0.4\%$ , respectively, showing rather efficient PL emissions. The PL decay curves of these two bands are shown in Fig. 2(b). The 500-nm PL band has long-lived components with lifetimes up to several tens of seconds, whereas the 400-nm PL band is mainly characterized by shorter lifetimes of several milliseconds. We should also note that the PLE spectra monitored at 400 and 500 nm are peaking at 260 and 257 nm, respectively. The PLE peak wavelengths and decay kinetics observed for the 500- and 400-nm PL bands are quite comparable to those observed for the  $F$  and  $F^+$  centers, respectively, in thermochemically reduced MgO [8,9]. To confirm that the PL observed in the present

sample is related to oxygen-ion vacancies, we annealed the MgO powders at temperatures up to  $1000^\circ\text{C}$  in an air atmosphere and measured the PL spectra of the annealed samples. As shown in Fig. 3, the original PL emission was decreased with increasing annealing temperature and completely extinguished after annealing at  $1000^\circ\text{C}$ . Thus, we attributed the observed 500- and 400-nm PL bands to the emission from two different oxygen-ion vacancies, namely,  $F$  and  $F^+$  centers, respectively. As for the blue-black substances that remained in the bottom of the crucible, no PL emission was observed. This indicates that the MgO crystals that remained in the crucible hardly contain  $F$  and  $F^+$  centers and are hence likely to be stoichiometric oxides.

In order to explore the possible stimulated emission from the colored MgO microcrystals, the power-dependent

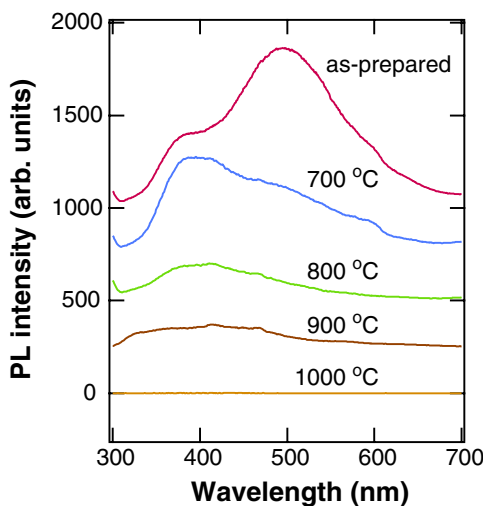


FIG. 3 (color online). PL spectra of the MgO powders deposited onto the lid before and after annealing in air. The annealing was performed for 1 h at the designated temperature. The excitation wavelength is 256 nm.

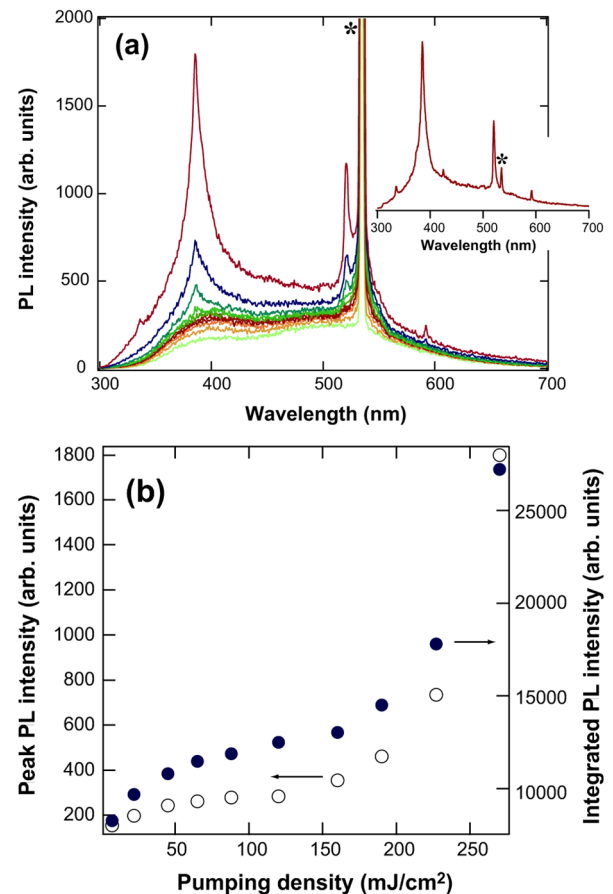


FIG. 4 (color online). Lasing characteristics of the MgO powders. (a) Emission spectra when the pumping density is (from bottom to top) 7, 22, 45, 65, 88, 120, 160, 190, 230, 270  $\text{mJ}/\text{cm}^2$ . The asterisk indicates the second harmonic (532 nm) of the Nd:YAG laser contaminated in the incident laser beam. The time-resolved emission spectrum (inset) is also shown to reduce the effect of contamination of the second harmonic light; the spectrum was obtained with a gate delay of 20 ns and a gate width of 5 ms at a pump density of 270  $\text{mJ}/\text{cm}^2$ . (b) The emission intensity at the peak wavelength (384 nm, open circles) and the wavelength-integrated intensity of emission (closed circles) as a function of the pump density.

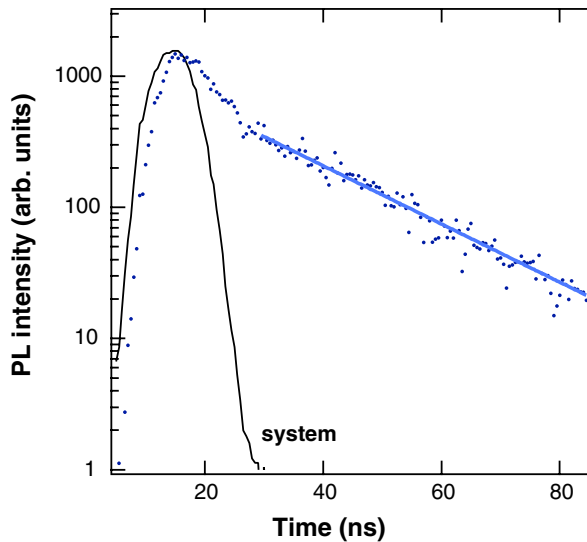


FIG. 5 (color online). The decay of the luminescence of the MgO powders at the peak wavelength (384 nm). The measurements were performed at the pump density of 250 mJ/cm<sup>2</sup>. A solid line is a pure exponential fit, yielding a decay time of 20 ns.

emission has been examined at room temperature (see Fig. 4). The pump beam was loosely focused on the powders that are placed in a silica cuvette in such a way that the beam diameter was reduced from  $\sim 10$  to  $\sim 3$  mm using an  $f = 150$ -mm lens. When the beam was more tightly focused on the sample, the sample was appreciably damaged and, accordingly, no stable PL emissions were observed. As shown in Figs. 4(a) and 4(b), the intensity of the  $F^+$  band at  $\sim 400$  nm preferentially increases with increasing pumping density. This behavior probably results from the amplified spontaneous emission, which is typically observed in high gain media owing to the preferential amplification of frequencies close to the maximum of the gain spectrum [15]. When the pumping density exceeds a threshold ( $\sim 160$  mJ/cm<sup>2</sup>), the  $F^+$  band becomes narrow and shows a rapid increase in intensity [see Fig. 4(a)], emerging a sharp peak at 384 nm. Time-resolved PL measurements (Fig. 5) demonstrate that the 384-nm peak exhibits a pure exponential decay with a decay time of 20 ns, which is much faster than the decay time of the spontaneous emission of the  $F^+$  band shown in Fig. 2(b). These observed effects, namely, strong narrowing of the emission, threshold nature of emission intensity, and major reduction in the decay time, all indicated that stimulated emission takes place from the  $F^+$  centers in the MgO powders. Well above the threshold, other sharp peaks emerge at 335, 423, 518, and 590 nm [see the inset of Fig. 4(a)], which are also characterized by a decay time of several tens of nanoseconds. The spectrally integrated emission intensity also shows a threshold behavior with respect to the pumping density [see Fig. 4(b)], implying that the stimulated emission occurs over a wide spectral region from  $\sim 350$  to  $\sim 600$  nm.

As mentioned earlier, no laser action has been reported from the  $F^+$  centers in MgO single crystals probably because of the diffusion, aggregation, and destruction of the color centers during the electronic excitation process. In the present MgO microcrystals, however, we suggest that some of the color centers are stabilized and immobilized at the boundaries of the crystalline grains, accounting for the stable laser emission even at room temperature. We also suggest that the well-faceted MgO microcrystals obtained in this work serve as natural resonance cavities and are hence responsible for the present lasing action without any fabricated mirrors. Previously, lasing from a resonator formed between the facets of nanocrystals and microcrystals has indeed been reported for various ZnO-based crystals [16]. However, we cannot completely exclude the possibility that the present laser action is induced by recurrent light scattering or random lasing [17]. This is because, as shown in Fig. 1(b), the present MgO microcrystals consist also of very fine, probably nanometer-sized, particles, which may induce recurring scattering in the powder. Further work needs to be done to clarify the physical origin of the laser emission from the present MgO microcrystals.

- 
- [1] G. Baldacchini, in *Spectroscopy and Dynamics of Collective Excitations in Solids*, edited by G. Di Bortolo (Plenum, New York, 1997), pp. 495–517.
  - [2] L.F. Mollenauer, in *Tunable Lasers*, edited by L.F. Mollenauer, J.C. White, and C.R. Pollock (Springer-Verlag, Berlin, 1992), 2nd ed., pp. 225–277.
  - [3] C.R. Pollock, J.F. Pinto, and E. Georgiou, *Appl. Phys. B* **48**, 287 (1989).
  - [4] B. Henderson, *Defects in Crystalline Solids* (Arnold, London, 1972), pp. 69–103.
  - [5] M.J. Weber, *Handbook of Lasers* (CRC Press, Boca Raton, FL, 2001), pp. 217–229.
  - [6] B. Henderson, *Opt. Lett.* **6**, 437 (1981).
  - [7] Y. Chen and R. Gonzalez, *Opt. Lett.* **10**, 276 (1985).
  - [8] G.H. Rosenblatt *et al.*, *Phys. Rev. B* **39**, 10 309 (1989).
  - [9] Y. Chen *et al.*, *Phys. Rev. B* **27**, 1276 (1983).
  - [10] M.S. Wrighton, D.S. Ginley, and D.L. A. Morse, *J. Phys. Chem.* **78**, 2229 (1974).
  - [11] *Binary Alloy Phase Diagrams*, edited by H. Okamoto, P.R. Subramanian, and L. Kacprzak (ASM International, Materials Park, OH, 1990), 2nd ed., Vol. 3, pp. 2531–2532.
  - [12] Y. Yin, G. Zhan, and Y. Xia, *Adv. Funct. Mater.* **12**, 293 (2002).
  - [13] U. Kahler and H. Hofmeister, *Appl. Phys. Lett.* **75**, 641 (1999).
  - [14] B.J. Hinds *et al.*, *J. Vac. Sci. Technol. B* **16**, 2171 (1998).
  - [15] W. Koechner and M. Bass, *Solid-State Lasers* (Springer, New York, 2003), pp. 141–143.
  - [16] M.H. Huang *et al.*, *Science* **292**, 1897 (2001); A.B. Djurišić *et al.*, *J. Phys. Chem. B* **109**, 19 228 (2005).
  - [17] H. Cao *et al.*, *Phys. Rev. Lett.* **82**, 2278 (1999).